

# XO-2b: a Prograde Planet with a Negligible Eccentricity, and an Additional Radial Velocity Variation\*

Norio NARITA,<sup>1</sup> Teruyuki HIRANO,<sup>2</sup> Bun'ei SATO,<sup>3</sup> Hiroki HARAKAWA,<sup>3</sup>  
Akihiko FUKUI,<sup>4,5</sup> Wako AOKI,<sup>1</sup> and Motohide TAMURA<sup>1</sup>

<sup>1</sup> National Astronomical Observatory of Japan, 2-21-1 Osawa, Mitaka, Tokyo, 181-8588, Japan

<sup>2</sup> Department of Physics, The University of Tokyo, Tokyo, 113-0033, Japan

<sup>3</sup> Department of Earth and Planetary Sciences, Tokyo Institute of Technology, Tokyo, 152-8550, Japan

<sup>4</sup> Okayama Astrophysical Observatory, National Astronomical Observatory,  
3037-5 Honjo, Kamogata, Asakuchi, Okayama 719-0232, Japan

<sup>5</sup> Solar-Terrestrial Environment Laboratory, Nagoya University, Nagoya, 464-8601, Japan  
norio.narita@nao.ac.jp

(Received 2011 August 22; accepted 2011 October 12)

## Abstract

We present precise radial velocities of XO-2 taken with the Subaru HDS, covering two transits of XO-2b with an interval of nearly two years. The data suggest that the orbital eccentricity of XO-2b is consistent with zero within  $2\sigma$  ( $e = 0.045 \pm 0.024$ ) and the orbit of XO-2b is prograde (the sky-projected spin-orbit alignment angle  $\lambda = 10^\circ \pm 72^\circ$ ). The poor constraint of  $\lambda$  is due to a small impact parameter (the orbital inclination of XO-2b is almost  $90^\circ$ ). The data also provide an improved estimate of the mass of XO-2b as  $0.62 \pm 0.02 M_{\text{Jup}}$ . We also find a long-term radial velocity variation in this system. Further radial velocity measurements are necessary to specify the cause of this additional variation.

**Key words:** stars: planetary systems: individual (XO-2) — stars: rotation — stars: binaries: general — techniques: radial velocities — techniques: spectroscopic

## 1. Introduction

Planetary orbits in binary systems provide useful clues to learn planetary migration mechanisms in binary systems. Planets in binary systems have a chance to take a different path of orbital migration than planets in single star systems. That is, due to the presence of a binary companion, an inner planet can evolve into a highly eccentric and highly tilted, or even retrograde orbit, by the mechanism known as the Kozai migration (Kozai 1962; Wu & Murray 2003; Fabrycky & Tremaine 2007; Lithwick & Naoz 2011; Katz et al. 2011). Observable evidences of the Kozai migration are large eccentricity and large spin-orbit misalignment of an inner planet. One can measure the orbital eccentricity via radial velocity (RV) measurements, and one can also learn the spin-orbit alignment angle at least in sky-projection via the Rossiter-McLaughlin effect (hereafter the RM effect: Rossiter 1924, McLaughlin 1924; Ohta et al. 2005; Hirano et al. 2010; Hirano et al. 2011a) in transiting systems.

One interesting example of a transiting planet in a wide binary system is HD 80606b, which has a large eccentricity ( $e = 0.93$ , Naef et al. 2001) and a large sky-projected spin-orbit alignment angle ( $\lambda = 42^\circ$ , Moutou et al. 2009; Pont et al. 2009; Winn et al. 2009b; Hébrard et al. 2010). The orbit of HD 80606b has been well explained by a scenario of the Kozai migration due to the presence of the binary

companion HD 80607 (Wu & Murray 2003). Another interesting example is WASP-8b, which has an eccentric and retrograde orbit with a wide binary companion (Queloz et al. 2010), although a Kozai migration scenario for WASP-8b has not been well examined. Other transiting planets in binary systems, however, show neither large eccentricity nor large spin-orbit misalignment (e.g., HD189733b: Bakos et al. 2006; Winn et al. 2006, TrES-4b: Mandushev et al. 2007; Narita et al. 2010b). This fact can be understood by considering that the Kozai migration needs to meet some stringent conditions (see e.g., Innanen et al. 1997; Wu et al. 2007; Narita et al. 2010c). To learn the occurrence frequency of the Kozai migration for planets in binary systems, it is important to increase the number of observations for such transiting systems.

We here report on the orbit of the transiting planet XO-2b, which was discovered by Burke et al. (2007) in the course of the XO survey. The host star XO-2 is a relatively faint ( $V = 11.18$ ) K0V star (the stellar mass  $0.98 \pm 0.02 M_{\text{s}}$  and the stellar radius  $0.97 \pm 0.02 R_{\text{s}}$ ) at  $\sim 150$  pc from the Sun (Burke et al. 2007). XO-2 has the twin (the same spectral type) stellar companion XO-2S at  $31''$  ( $\sim 4600$  AU) separation. We note that the Kozai migration for XO-2b could occur if the eccentricity of the binary orbit (currently unknown) is very large ( $e \geq 0.9$ ), when the timescale of the Kozai migration is shorter than the timescale of a perturbation due to General Relativity for XO-2b (Wu et al. 2007). Burke et al. (2007) reported the mass, radius, orbital period of XO-2b as  $0.57 \pm 0.06 M_{\text{Jup}}$ ,  $0.98_{-0.01}^{+0.03} R_{\text{Jup}}$ , and  $P = 2.615857 \pm 0.000005$  days, respec-

\* Based on data collected at Subaru Telescope, which is operated by the National Astronomical Observatory of Japan.

tively. The eccentricity of XO-2b was assumed to be zero in the discovery paper, and no measurement of the RM effect in this system has been reported. In this letter, we present RVs of XO-2 spanning about two years and covering two full transits of XO-2b allowing us to model the RM effect. Our RV data suggest a small eccentricity and a likely spin-orbit alignment of XO-2b, concluding no supporting evidence of the Kozai migration. In addition, we find a long-term RV trend for XO-2. This RV acceleration may suggest a third body in this system.

The rest of this letter is organized as follows. We present details of our observations and reductions of RV data in section 2. We describe our model to fit the observed data in section 3. We present our results on the orbit of XO-2 and discussions on possible migration mechanisms of XO-2b in section 4. Finally, we summarize the findings of this letter in section 5.

## 2. Observations and Data Reductions

We observed XO-2 with the standard I2a setup of the High Dispersion Spectrograph (HDS; Noguchi et al. 2002) onboard the Subaru 8.2m telescope on Mauna Kea. An iodine gas absorption cell was inserted for RV measurements. We measured RVs around two full transits of XO-2b on UT 2008 March 9 and UT 2009 November 24. We also gathered out-of-transit RVs spanning about two years from 2008 to 2010. Slit width was either  $0''.4$  ( $R = 90000$ ) or  $0''.6$  ( $R = 60000$ ) depending on observing conditions. Exposure times were 600 s for around-transit phase and 900 s for out-of-transit phase. Finally, we obtained a high signal-to-noise ratio (SNR over 200) and high spectral resolution ( $R = 90000$ ) template spectrum on UT 2011 February 15 with an exposure time of 1800 s.

We process the observed frames with standard IRAF procedures and extract 1D spectra. Relative RVs and uncertainties are computed by the algorithm of Butler et al. (1996) and Sato et al. (2002). We estimate the uncertainty of each RV based on the scatter of RV solutions for  $\sim 4 \text{ \AA}$  segments of each spectrum as described in Narita et al. (2007). The RVs and internal errors are summarized in table 1, and plotted in the top panel of figure 1. Note that we use HJD<sub>UTC</sub> (Heliocentric Julian Date in the Coordinated Universal Time) as a time standard.

Since we do not have good photometric transit data, we additionally incorporate five published photometric light curves taken with Keplercam on the 1.2m telescope at the Fred Lawrence Whipple Observatory (FLWO) on Mount Hopkins, Arizona (Fernandez et al. 2009). Those transits were observed in the Sloan  $z'$  band. Following the procedure by Fernandez et al. (2009) and Narita et al. (2010a), we rescale the photometric uncertainties to account for time-correlated noise (so-called red noise: see e.g., Pont et al. 2006) by calculating a red noise factor  $\beta = \sigma_{N,\text{obs}}/\sigma_{N,\text{ideal}}$  for various  $N$  (corresponding to 10-20 min), and multiply the photometric uncertainties of each dataset by the maximum value of  $\beta$ . We note that we find slightly higher values of  $\beta$  than Fernandez et al. (2009), and thus our photometric uncertainties are conservative.

## 3. Model

First we model the RVs assuming a single orbiting planet. We then find RVs around the second transit are vertically off by about  $15 \text{ m s}^{-1}$  from those around the first transit (see the middle panel of figure 2). We also find that residuals from the single planet model has a linear trend in time (see the middle panel of figure 1). We thus model our data assuming a single orbiting planet with a linear RV acceleration. The five FLWO transit light curves are simultaneously fitted assuming the quadratic limb-darkening law. We note that we fix one coefficient ( $u_1$ ) of the limb-darkening parameters to  $u_1 = 0.25$ , which is the central value derived by Fernandez et al. (2009). This treatment is useful so as to avoid underestimate of uncertainties for fitted parameters (see Southworth 2008).

Consequently, our model has 16 free parameters: the RV semiamplitude  $K$ , the eccentricity  $e$ , the argument of periastron  $\varpi$ , the sky-projected stellar rotational velocity  $V \sin I_s$ , the sky-projected spin-orbit alignment angle  $\lambda$ , the offset RV for the Subaru data  $\gamma$ , the RV acceleration  $\dot{\gamma}$ , the planet-star radii ratio  $R_p/R_s$ , the orbital inclination  $i$ , the semi-major axis in units of the stellar radius  $a/R_s$ , one of the limb-darkening coefficients  $u_2$ , and the five mid-transit times of the FLWO data  $T_c(E)$ . We fix  $P = 2.6158640$  days and  $T_c(0) = 2454466.88467$  in HJD<sub>UTC</sub> which are the values reported by Fernandez et al. (2009). Uncertainties of mid-transit times for the two spectroscopic transit observations (UT 2008 March 9 and UT 2009 November 24) are well within the shortest exposure time of RVs (600 s) and have little effect on results.

The  $\chi^2$  statistic for the joint fit is

$$\chi^2 = \sum_i \left[ \frac{f_{i,\text{obs}} - f_{i,\text{model}}}{\sigma_i} \right]^2 + \sum_j \left[ \frac{v_{j,\text{obs}} - v_{j,\text{model}}}{\sigma_j} \right]^2,$$

where  $f_{i,\text{obs}}$ ,  $v_{j,\text{obs}}$ ,  $\sigma_i$ , and  $\sigma_j$  are the observed relative fluxes, RVs, and their uncertainties. We note that we do not add RV jitter in  $\sigma_j$ , since reduced  $\chi^2$  for the RV data is below unity as shown later (see table 2). The modeled fluxes ( $f_{i,\text{calc}}$ ) are computed by the formula given by Ohta et al. (2009), and the modeled RVs ( $v_{j,\text{model}}$ ) are calculated as  $v_{\text{calc}} = v_{\text{Kepler}} + v_{\text{RM}} + \dot{\gamma}t + \gamma$ , where  $v_{\text{Kepler}}$  is the Keplerian motion,  $v_{\text{RM}}$  is the RM effect, and  $\dot{\gamma}t$  represents the long-term RV trend. We compute the RM effect  $v_{\text{RM}}$  by the accurate analytic formula for a K0V star described in Hirano et al. (2011a). In the formula, we use  $u_1 = 0.714$  and  $u_2 = 0.114$  for the band of the iodine absorption lines, based on the table of Claret (2004). We then determine optimal parameter values by minimizing the  $\chi^2$  statistic using the AMOEBA algorithm (Press et al. 1992). Uncertainties of free parameters are estimated by the criterion  $\Delta\chi^2 = 1.0$ .

## 4. Results and Discussions

The best-fit parameters and errors are summarized in table 2. Photometric parameters related with only the FLWO data ( $R_p/R_s$ ,  $u_2$ , and  $T_c$ ) are essentially consis-

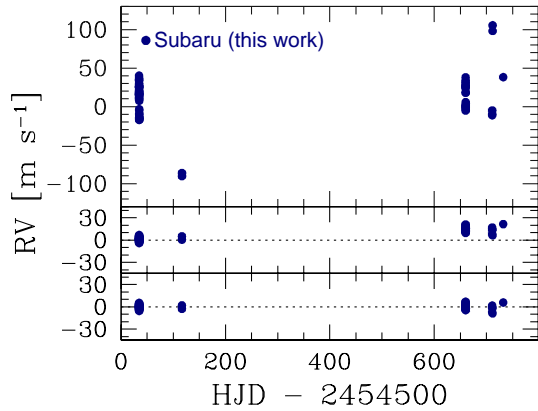


**Fig. 1.** Top panel: RVs of XO-2 observed with the Subaru HDS. Middle panel: Residuals of RVs from the best-fit model without subtracting the long-term RV trend. Bottom panel: Same as the middle panel but with subtracting the RV trend.

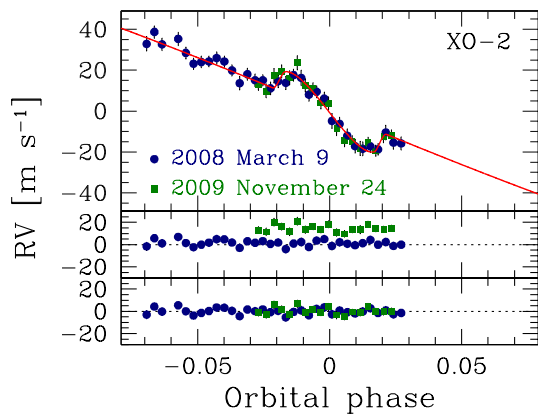


**Fig. 2.** Top panel: Phased RVs around transits after subtracting the RV trend. The circle and square symbols represent RVs on UT 2008 March 9 and UT 2009 November 24, respectively. Middle panel: Residuals of RVs from the best-fit model without subtracting the long-term RV trend. Bottom panel: Same as the middle panel but with subtracting the RV trend.

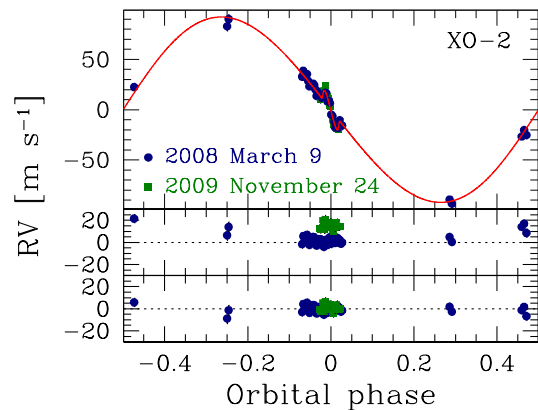


**Fig. 3.** The same as figure 2, but for a whole orbital phase.

tent with the results of Fernandez et al. (2009) and are not shown. Figure 1 plots the Subaru RVs (the top panel), residuals from the best-fit model without (the middle panel) and with (the bottom panel) a subtraction of the RV trend  $\dot{\gamma}t$ . The  $\chi^2$  for 59 RVs is 48.8 and the rms of RVs is  $3.08 \text{ m s}^{-1}$ . This validates our treatment of stellar jitter in the RV errors. We find that the RV semi-amplitude  $K$  ( $92.2 \pm 1.7 \text{ m s}^{-1}$ ) is about 8% larger than the value ( $85 \pm 8 \text{ m s}^{-1}$ ) reported by Burke et al. (2007) with a smaller uncertainty. This provides an improved estimate of the mass of XO-2b as  $0.62 \pm 0.02 M_{\text{Jup}}$ . We also find the eccentricity of XO-2b is small and consistent with zero within about  $2\sigma$ . We note that the results and errors are essentially unchanged even if we jointly fit the RV data by Burke et al. (2007).

Figure 2 shows phased RVs around the transit phase with the best-fit model. The RV trend is subtracted in the top and bottom panels, but not subtracted in the middle panel. Figure 3 is the same as figure 2, but for a whole orbital phase. The shape of the RM effect clearly suggests a prograde orbit of XO-2. However, the derived constraint on  $\lambda$  is very poor, namely  $\lambda = 10^\circ \pm 72^\circ$ . It is because the orbital inclination  $i$  of XO-2b is near  $90^\circ$ . Figure 4 plots a  $\Delta\chi^2$  contour map in  $(\lambda, V \sin I_s)$  space. Our best-fit value of  $V \sin I_s$  based on the RM effect is  $1.45 \text{ km s}^{-1}$ , which is in good agreement with a value  $1.4 \pm 0.3 \text{ km s}^{-1}$  derived by Burke et al. (2007) based on a spectroscopic line analysis. Schlafman (2010) independently estimated  $V \sin I_s$  of XO-2 as  $1.69 \pm 0.2 \text{ km s}^{-1}$  based on its mass and age, and concluded that the XO-2 system is likely to be aligned. The conclusion is apparently consistent with our result. Thus although a larger value of  $V \sin I_s$  is allowed by the RM effect, such a larger  $V \sin I_s$  is unlikely when considering the other analyses. As a test case, if we add a prior constraint  $1.4 \pm 0.3 \text{ km s}^{-1}$  to the  $\chi^2$  statistic, we find  $\lambda = 9^\circ_{-34^\circ}^{+26^\circ}$ . Thus the orbit of XO-2b is unlikely to be highly tilted, but an exact value of  $\lambda$  is unfortunately indeterminate. As a result, we conclude a small eccentricity and a likely spin-orbit alignment for the orbit of XO-2b. As is known today, RM measurements have shown that about two thirds of close-in giant planets are spin-orbit aligned and prograde, whereas the last third is strongly misaligned or even retrograde (e.g., Hébrard et al. 2011). Our result suggests that XO-2b is apparently in the first category.

We determine the RV acceleration of XO-2 as  $\dot{\gamma} = 7.51 \pm 0.58 \text{ m s}^{-1} \text{ yr}^{-1}$ . The trend is small but significant in the two years. If we do not include  $\dot{\gamma}$  as a free parameter, the  $\chi^2$  value for the RVs changes from 48.8 to 231.9. Assuming a long-term linear trend, this RV acceleration can be explained by a hypothetical third body (index “c”) whose mass and orbit follow a relation  $M_c \sin i_c / a_c^2 = 0.042 \pm 0.003 M_{\text{Jup}} \text{ AU}^{-2}$ . The orbital period of the third body can be longer than  $\sim 8 \text{ yr}$  ( $\sim 4 \text{ AU}$ ) since the RV trend is apparently linear spanning about 2 years. For example, a  $1 M_{\text{Jup}}$  planet at 5 AU like the Jupiter in our Solar System meets the relation. We note that the binary companion XO-2S does not meet this relation. There is another possibility that the timescale of

the additional RV variation is a few hundred days, due to the lack of our observations between the two transits. Additional RV measurements with the Subaru HDS will allow us to discriminate the timescale of the RV variation.

Other possibilities of the trend include a systematic RV variation of the Subaru HDS, starspots or magnetic cycles of XO-2. The first scenario is unlikely, because RVs of the Subaru HDS for RV standard stars are stable within a few  $\text{m s}^{-1}$  (Harakawa et al. 2010; Sato et al. 2009). The starspot scenario is also unlikely, because no significant RV variation has been observed for XO-2 in a timescale corresponding to the rotation period of the host star ( $\sim 35$  day: Matsumura et al. 2010), although RV variations caused by spots should have been maximum. At this point, we cannot exclude the possibility of magnetic cycles of XO-2 recently examined by Lovis et al. (2011), although any strong magnetic activity has not been reported for this system. To specify the cause of the RV variation and make a decisive conclusion, further RV monitoring would be very important in this system.

There is still a possibility that the mutual inclination between the orbital axes of the transiting planet XO-2b and the binary companion XO-2S was once larger than the threshold value of the Kozai mechanism. In addition, if the eccentricity of the binary orbit is larger than  $\sim 0.9$ , the timescale of the Kozai migration might have been shorter than that of General Relativity for XO-2b at the birthplace ( $\sim 2$  Gyr based on Wu & Murray 2003). However, the presence of the hypothetical third body completely dictates that XO-2b cannot be migrated through the Kozai migration caused by XO-2S, since the gravitational perturbation timescale due to the third body (comparable to the orbital period of the third body) is much shorter than the Kozai migration timescale (see e.g., Innanen et al. 1997; Narita et al. 2010c).

On the other hand, Winn et al. (2010) pointed out that a hot Jupiter around a cool (less than  $\sim 6250\text{K}$ ) star can lead to a re-alignment of its spin-orbit alignment angle due to the tidal force on a convective surface layer of the cool host star. XO-2 is in the category of a cool star ( $\sim 5340\text{K}$ : Burke et al. 2007) and the spin axis of the host star might have been re-aligned. Thus one possible migration scenario is that XO-2b has migrated through planet-planet scattering (e.g., Rasio & Ford 1996; Nagasawa et al. 2008; Chatterjee et al. 2008), and subsequently the eccentricity and the spin-orbit alignment angle have been damped. In that case, the hypothetical third body may be the counterpart of the planet-planet scattering. Another possible migration mechanism is the standard disk-planet interaction mechanism (e.g., Lin et al. 1996; Ida & Lin 2004). Although we cannot specify the migration mechanism of XO-2b at this point in time, further measurements of transit timings of XO-2b would be useful to constrain another low-mass body in mean motion resonance, which can be an evidence of the disk-planet migration (Fernandez et al. 2009). Any detection or constraint of such a mean motion resonance body by transit timings, as well as further RV measurements, would allow further discussions on the migration history of this system.

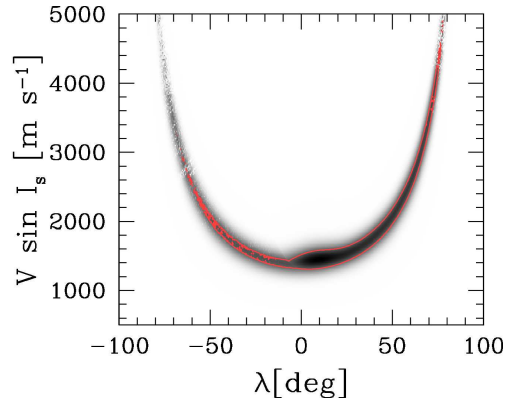


**Fig. 4.** A  $\chi^2$  contour map in  $\lambda$ - $V \sin I_s$  space. The solid lines represent contour for  $\Delta\chi^2 = 1.0$ .

## 5. Summary

We have monitored RVs of XO-2 spanning about two years with the Subaru HDS. We find a small eccentricity and a likely spin-orbit alignment for the orbit of the transiting planet XO-2b, and we also detect a long-term RV acceleration of the host star. Based on the observed properties of this system, we constrain the Kozai migration scenario of XO-2b. This illustrates that a presence of a wide binary companion does not necessarily suggest the Kozai migration (see also Narita et al. 2009; Winn et al. 2009a; Narita et al. 2010c, for the migration mechanism of a retrograde planet HAT-P-7b). To constrain the occurrence frequency of the Kozai migration for planets in binary systems, combinations of observations of (1) the orbital eccentricity by RV measurements, (2) the spin-orbit alignment angle by the RM effect, and (3) the binarity (or multiplicity) of the system by high-contrast direct imaging, are of special importance. Accumulating those observations for transiting planetary systems would allow us to learn more about planetary migration mechanisms in the future.

This letter is based on data collected at Subaru Telescope, which is operated by the National Astronomical Observatory of Japan. We acknowledge a kind support by Akito Tajitsu for the Subaru HDS observations. We are grateful for Zach Gazak for helpful discussions on XO-2 photometric observations. The data analysis was in part carried out on common use data analysis computer system at the Astronomy Data Center, ADC, of the National Astronomical Observatory of Japan. N.N. acknowledges a support by NINS Program for Cross-Disciplinary Study. T.H. is supported by a Japan Society for Promotion of Science (JSPS) Fellowship for Research (DC1: 22-5935). M.T. is supported by the Ministry of Education, Science, Sports and Culture, Grant-in-Aid for Specially Promoted Research, 22000005. We wish to acknowledge the very significant cultural role and reverence that the summit of Mauna Kea has always had within the indigenous people in Hawai'i.

**References**

- Bakos, G. Á., Pál, A., Latham, D. W., Noyes, R. W., & Stefanik, R. P. 2006, *ApJL*, 641, L57
- Burke, C. J., et al. 2007, *ApJ*, 671, 2115
- Butler, R. P., Marcy, G. W., Williams, E., McCarthy, C., Dosanji, P., & Vogt, S. S. 1996, *PASP*, 108, 500
- Chatterjee, S., Ford, E. B., Matsumura, S., & Rasio, F. A. 2008, *ApJ*, 686, 580
- Claret, A. 2004, *A&A*, 428, 1001
- Fabrycky, D., & Tremaine, S. 2007, *ApJ*, 669, 1298
- Fernandez, J. M., Holman, M. J., Winn, J. N., Torres, G., Shporer, A., Mazeh, T., Esquerdo, G. A., & Everett, M. E. 2009, *AJ*, 137, 4911
- Fukui, A., et al. 2011, *PASJ*, 63, 287
- Harakawa, H., et al. 2010, *ApJ*, 715, 550
- Hébrard, G., et al. 2010, *A&A*, 516, A95+
- Hébrard, G., et al. 2011, *A&A*, 527, L11+
- Hirano, T., Suto, Y., Taruya, A., Narita, N., Sato, B., Johnson, J. A., & Winn, J. N. 2010, *ApJ*, 709, 458
- Hirano, T., et al. 2011, *ApJ* in press, arXiv:1108.4430
- Ida, S., & Lin, D. N. C. 2004, *ApJ*, 616, 567
- Innanen, K. A., Zheng, J. Q., Mikkola, S., & Valtonen, M. J. 1997, *AJ*, 113, 1915
- Katz, B., Dong, S., & Malhotra, R. 2011, arXiv:1106.3340
- Kozai, Y. 1962, *AJ*, 67, 591
- Lin, D. N. C., Bodenheimer, P., & Richardson, D. C. 1996, *Nature*, 380, 606
- Lithwick, Y., & Naoz, S. 2011, arXiv:1106.3329
- Lovis, C., et al. 2011, arXiv:1107.5325
- Mandushev, G., et al. 2007, *ApJL*, 667, L195
- Matsumura, S., Peale, S. J., & Rasio, F. A. 2010, *ApJ*, 725, 1995
- McLaughlin, D. B. 1924, *ApJ*, 60, 22
- Moutou, C., et al. 2009, *A&A*, 498, L5
- Naef, D., et al. 2001, *A&A*, 375, L27
- Nagasawa, M., Ida, S., & Bessho, T. 2008, *ApJ*, 678, 498
- Narita, N., Hirano, T., Sanchis-Ojeda, R., Winn, J. N., Holman, M. J., Sato, B., Aoki, W., & Tamura, M. 2010a, *PASJ*, 62, L61+
- Narita, N., Sato, B., Hirano, T., & Tamura, M. 2009, *PASJ*, 61, L35
- Narita, N., Sato, B., Hirano, T., Winn, J. N., Aoki, W., & Tamura, M. 2010b, *PASJ*, 62, 653
- Narita, N., et al. 2007, *PASJ*, 59, 763
- Narita, N., et al. 2010c, *PASJ*, 62, 779
- Noguchi, K., et al. 2002, *PASJ*, 54, 855
- Ohta, Y., Taruya, A., & Suto, Y. 2005, *ApJ*, 622, 1118
- Ohta, Y., Taruya, A., & Suto, Y. 2009, *ApJ*, 690, 1
- Pont, F., Zucker, S., & Queloz, D. 2006, *MNRAS*, 373, 231
- Pont, F., et al. 2009, *A&A*, 502, 695
- Press, W. H., Teukolsky, S. A., Vetterling, W. T., & Flannery, B. P. 1992, *Numerical recipes in C. The art of scientific computing* (Cambridge: University Press, —c1992, 2nd ed.)
- Queloz, D., et al. 2010, *A&A*, 517, L1+
- Rasio, F. A., & Ford, E. B. 1996, *Science*, 274, 954
- Rossiter, R. A. 1924, *ApJ*, 60, 15
- Sato, B., Kambe, E., Takeda, Y., Izumiura, H., & Ando, H. 2002, *PASJ*, 54, 873
- Sato, B., et al. 2009, *ApJ*, 703, 671
- Schlaufman, K. C. 2010, *ApJ*, 719, 602
- Southworth, J. 2008, *MNRAS*, 386, 1644
- Winn, J. N., Fabrycky, D., Albrecht, S., & Johnson, J. A. 2010, *ApJL*, 718, L145
- Winn, J. N., Johnson, J. A., Albrecht, S., Howard, A. W., Marcy, G. W., Crossfield, I. J., & Holman, M. J. 2009a, *ApJL*, 703, L99
- Winn, J. N., et al. 2006, *ApJL*, 653, L69
- Winn, J. N., et al. 2009b, *ApJ*, 703, 2091
- Wu, Y., & Murray, N. 2003, *ApJ*, 589, 605
- Wu, Y., Murray, N. W., & Ramsahai, J. M. 2007, *ApJ*, 670, 820

**Table 1.** RV data taken with the Subaru HDS.

SUbaru HDS RVs		
Time [HJD-UTC]	Value [m s <sup>-1</sup> ]	Error [m s <sup>-1</sup> ]
2454534.71592	0.00	3.53
2454534.72354	5.83	3.09
2454534.73116	-0.19	3.03
2454534.74713	2.47	3.28
2454534.75474	-4.44	2.92
2454534.76237	-9.72	2.68
2454534.76999	-8.87	2.88
2454534.77761	-8.62	2.73
2454534.78523	-6.95	3.11
2454534.79284	-8.66	2.85
2454534.80046	-12.98	2.82
2454534.80807	-19.25	3.35
2454534.81570	-14.86	2.92
2454534.82333	-17.81	3.20
2454534.83095	-17.81	2.76
2454534.83856	-21.79	3.16
2454534.84618	-18.34	3.07
2454534.85380	-19.09	3.19
2454534.86141	-15.27	2.89
2454534.86904	-16.67	3.85
2454534.87665	-24.82	3.32
2454534.88427	-23.42	3.00
2454534.89188	-26.77	3.12
2454534.89949	-37.70	3.60
2454534.90711	-39.15	3.17
2454534.91472	-44.97	3.35
2454534.92234	-50.05	3.42
2454534.92996	-51.32	3.43
2454534.93759	-50.14	3.05
2454534.94520	-51.64	2.84
2454534.95282	-43.37	3.53
2454534.96043	-48.30	3.25
2454534.96805	-48.68	3.22
2454616.73649	-120.61	3.04
2454616.75121	-124.63	3.02
2455160.01806	-6.98	2.87
2455160.02580	-10.17	3.44
2455160.03354	-2.75	3.50
2455160.04127	-0.66	3.28
2455160.04900	-3.77	3.53
2455160.05675	3.62	3.52
2455160.06449	-7.39	3.23
2455160.07224	-8.94	2.90
2455160.07999	-16.07	2.96
2455160.08773	-16.25	3.23
2455160.09570	-28.54	3.52
2455160.10344	-34.43	2.95
2455160.11118	-34.92	2.78
2455160.11893	-38.27	3.51
2455160.12668	-35.58	2.85
2455160.13442	-39.42	2.75
2455160.14217	-32.60	2.98
2455160.14991	-32.10	2.83
2455210.99190	-45.61	3.11
2455211.00660	-39.25	2.88
2455211.02128	-44.23	3.70
2455211.75316	63.93	4.56
2455211.76263	71.23	4.44
2455232.09437	3.96	3.67

\* All data are presented in the electric table.

**Table 2.** Best-fit values and errors of the parameters.

Free Parameter	Value	Error
$K$ [m s <sup>-1</sup> ]	92.2	±1.7
$e$	0.045	±0.024
$\varpi$ [°]	270	$^{+10}_{-7}$
$V \sin I_s$ [km s <sup>-1</sup> ]	1.45	$^{+2.73}_{-0.14}$
$\lambda$ [°]	10	±72
$i$ [°]	88.7	$^{+1.3}_{-0.9}$
$a/R_s$	8.43	$^{+0.32}_{-0.34}$
$\gamma$ [m s <sup>-1</sup> ]	-34.3	±1.1
$\dot{\gamma}$ [m s <sup>-1</sup> yr <sup>-1</sup> ]	7.51	±0.58
Derived Parameter	Value	Error
$M_p$ [ $M_{\text{Jup}}$ ]	0.62	±0.02
$M_c \sin i_c / a_c^2$ [ $M_{\text{Jup}} \text{ AU}^{-2}$ ]	0.042	±0.003
$\chi^2$ for 59 RVs	48.8	–
rms [m s <sup>-1</sup> ]	3.08	–